Biochimica et Biophysica Acta 1818 (2012) 1205–1210

Contents lists available at SciVerse ScienceDirect

Biochimica et Biophysica Acta

journal homepage: www.elsevier.com/locate/bbamem

Membrane models of *E. coli* containing cyclic moieties in the aliphatic lipid chain

Kunal R. Pandit, Jeffery B. Klauda *

Department of Chemical and Biomolecular Engineering, University of Maryland, College Park, MD 20742, USA

ARTICLE INFO

Article history:
Received 9 November 2011
Received in revised form 9 January 2012
Accepted 10 January 2012
Available online 18 January 2012

Keywords:
E. coli membranes
Hydrophobic mismatch
Molecular simulations
Force field development

ABSTRACT

Nearly all molecular dynamics simulations of bacterial membranes simplify the lipid bilayer by composing it of only one or two lipids. Previous attempts of developing a model *E. coli* membrane have used only 1-palmitoyl-2-oleoyl-*sn*-glycero-3-phosphoethanolamine (POPE) and (1-palmitoyl-2-oleoyl-*sn*-glycero-3-phosphoglycerol) POPG lipids. However, an important constituent of bacterial membranes are lipids containing a cyclopropane ring within the acyl chain. We have developed a complex membrane that more accurately reflects the diverse population of lipids within *E. coli* cytoplasmic membranes, including lipids with a cyclic moiety. Differences between the deuterium order profile of cyclic lipids and monounsaturated lipids are observed. Furthermore, the inclusion of the cyclopropane ring decreases the surface density of the bilayer and produces a more rigid membrane as compared to POPE/POPG membranes. Additionally, the diverse acyl chain length creates a thinner bilayer which matches the hydrophobic thickness of *E. coli* transmembrane proteins better than the POPE/POPG bilayer. We believe that the complex lipid bilayer more accurately describes a bacterial membrane and suggest the use of it in molecular dynamic simulations rather than simple POPE/POPG membranes.

1. Introduction

The complexity of biological membranes is immense due to a heterogeneous mixture of various biomolecules. The simplest description would just be a homogenous lipid bilayer. A more realistic model would include a variety of lipids, sterols, and membrane proteins. Furthermore, a complete portrayal would have glycosylated lipids, proteins, and cytoskeleton components. Understandably, a complete description is impractical to use in most studies, but a simple homogeneous lipid bilayer may be an insufficient model.

An accurate representation of the membrane environment is important because lipid–protein interactions are essential to membrane protein function and orientation. Loss of these interactions may destabilize and inactivate the protein. Even substituting the lipid environment with detergents may be inadequate as lost protein functionality has been experimentally observed [1]. Lipids may also play an integral role in a protein's mechanism. Krämer and Ziegler [2] have crystallized a structure of BetP where a lipid interaction aids in regulating its function. Lensik et al. [3] found a 1-palmitoyl-2-oleoyl-*sn*-glycero-3-phosphoethanolamine (POPE) mediated a salt bridge involved in proton gradient-sensing of the integral membrane protein lactose permease. The function of mechanosensitive channels, such as MscS and MscL are controlled by the surface tension in the lipid bilayer [4].

Model membranes consist of a simple lipid bilayer composed of the most relevant lipids. Experimentally, unilamellar vesicles are formed from either a distribution of naturally derived lipids [5] or a mixture of specific lipids and sterols. In explicit molecular dynamics (MD) simulations, membranes usually only consist of one or two different lipids and may include sterols. Recently, detailed membranes consisting of a more diverse lipid population has been developed to model Chlamydia and Yeast membranes [6,7]. With MD simulations of bacterial membrane proteins, it is common to use a membrane consisting of only POPE [8] and in some cases in combination with 1-palmitoyl-2-oleoyl-*sn*-glycero-3-phosphoglycerol (POPG) lipids. This is due to the ease of generating such a membrane, for example through CHARMM-GUI [9]. Investigators conveniently focus their efforts on studying the protein, leaving the membrane as an afterthought. However, the composition of bacterial membranes varies depending on the bacterial species, strain, nutrients, and growth phase [10].

The goal of this study was to develop an accurate representation of an *E. coli* cytoplasmic membrane for use in further simulation studies. It has routinely been found that bacterial membranes are mainly composed of phosphoethanolamine (PE) and phosphoglycerol (PG) lipids. Murzyn et al. [11] previously developed an *E. coli* computer model membrane with a 3:1 POPE:POPG lipid bilayer. Zhao et al. [12] also developed a 3:1 POPE:POPG membrane to study the role of PG lipids in stabilizing bacterial membranes. An important constituent of several bacterial membranes are lipids with a cyclic moiety [13,14], which have been neglected in previous works. Quantum Mechanical (QM) based parameters for the cyclic moiety were

* Corresponding author. Tel.: +1 301 405 1320; fax: +1 301 314 9126.
E-mail address: jbklauda@umd.edu (J.B. Klauda).

0005-2736/$ – see front matter © 2012 Elsevier B.V. All rights reserved.
doi:10.1016/j.bbamem.2012.01.009

developed and tested against available data in the literature. Then, a model *E. coli* membrane consisting of saturated, unsaturated, and cyclic-containing lipids was developed along with a standard POPE/POPG model for comparison. Deuterium order parameter (S_{CD}) profiles were calculated for evaluation of the force field parameters. The thickness of the membranes was measured from their respective electron density profiles (EDP). Finally, the surface area per lipid and area compressibility modulus was calculated to evaluate bulk properties of the membranes.

2. Methods

2.1. Model E. coli membrane composition

QM-based parameters were developed to describe the cyclic moiety of 1-palmitoyl-2-*cis*-9,10-methylene-hexadecanoic-acid-*sn*-glycero-3-phosphoethanolamine (PMPE). Details regarding the parameters fit to QM calculations can be found in the Supplementation materials and in Table S1. The *sn*-2 fatty acid chain was numbered 1–16 down the main chain and the extended carbon numbered 17, forming the cyclic moiety between C9 and C10 (see Fig. 1). A pure PMPE membrane consisting of 76 lipids per leaflet was generated to evaluate the force field parameters. All membranes studied had about 30:1 water to lipid ratio (Table 1).

To develop the model *E. coli* membranes, it was decided to focus on a K12 strain based on the data available in the literature. Our standard POPE/POPG only membrane consisted of 76 lipids per leaflet in about a 5:1 POPE:POPG. The larger PE:PG compared to previous simulation studies [11,12] was based on the lipid composition of K12 CSH2 *E. coli* harvested in log phase and analyzed using gas chromatography [15].

A combination of two independent studies was used to define the lipid composition of the complex membrane referred to as Top6. In one, the relative composition of lipid mass:charge (m/z) ratios of a LM 3118 K12 *E. coli* was found using a liquid chromatography/electrospray ionization tandem mass spectrometry technique [16]. However, some m/z species could be accounted for by different combinations of fatty acid chains at the *sn*-1 or *sn*-2 position. In the other study, the fatty acid composition of NBRC 3301 K12 *E. coli* was determined using two different but complementary analyses; thermally assisted hydrolysis and methylation-gas chromatography (THM-GC) and matrix-assisted laser desorption/ionization mass spectrometry (MALDI-MS) [17]. The fatty acid composition data was used to estimate the fraction of each fatty acid combination in the m/z population.

The composition of the Top6 membrane consisted of the 6 most abundant lipids (Table S2). The PE to PG ratio within the membrane was about 4:1 with 78 lipids per leaflet. The percentage of the fatty acid chains 15:0, cy17:0, 16:0, 16:1, and 18:1 in the membrane were 7%, 35%, 40%, 8%, and 10% respectively. Cardiolipin was excluded from the membrane because experimentally it was found to be in low concentrations (~1 to 2%) [15]. It should be noted though, that cardiolipin is an important component of an *E. coli* membrane in the polar and septal regions of the bacterium [18] and thus our model should not be used for these regions.

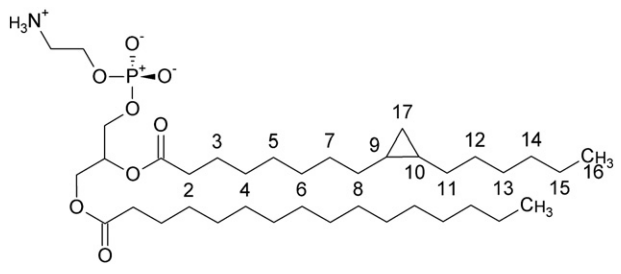

Fig. 1. Structure of PMPE. The backbone of the *sn-2* chain is numbered 1–16 and the protruding carbon which forms the cyclopropane ring is numbered 17.

Table 1
Compositions of model membranes.

Membrane	PE:PG	Water:lipid	Total lipids	Total atoms
POPE/POPG	5.3:1	32.7	152	32,222
PMPE	1:0	31.8	152	32,223
Top6	4.2:1	32.8	156	33,134

2.2. Simulation and analysis

Coordinates for all membranes were taken from membranes developed through CHARMM-GUI [9] (see Table 1 for details). Missing coordinates were generated in CHARMM [19]. CHARMM-GUI scripts for minimization and equilibration of bilayers were also carried out in CHARMM. Care was taken to restrain *cis* double bonds and *cis* cyclopropane rings during minimization.

NAMD [20] and CHARMM programs were used to perform isothermic–isobaric ensemble (NPT) simulations of the bilayers. All simulations were performed under the following protocol. A Lennard–Jones force-based switching function over 8 to 12 Å was implemented. Particle Mesh Ewald [21] was used for long-range electrostatics. Membranes were simulated for 50 ns with 2 fs time steps. Hydrogen atoms were constrained using the SHAKE [22] algorithm. The temperature and pressure were held at 310.15 K and 1 bar, respectively. In the CHARMM simulation, temperature and pressure control was achieved with a Hoover thermostat [23] and Nosé-Hoover piston respectively [24]. In NAMD simulations, temperature and pressure control was achieved through a Langevin Piston [25]. Each membrane composition was simulated 3 times using the cyclic modified CHARMM36 (C36) force field [26].

Upon completion of the simulations the trajectories were analyzed to compute overall surface areas per lipid, deuterium order parameters, electron density profiles, compressibility moduli, and compression energy density. The surface area per lipid (box length squared divided by number of lipids per leaflet) gave a general idea of the packing of the lipids within the xy plane. It was also tracked to monitor whether the simulation was in equilibrium. The deuterium order parameters (S_{CD}) of the acyl chain are a measure of the C – H vector order. As the order parameter increases the chain order increases as well. Broadly speaking, the order parameter is expected decreased down the acyl chain. The S_{CD} of each C – H vector was calculated as follows

$$S_{CD} = \left|\frac{3}{2}\cos^2\beta - \frac{1}{2}\right| \quad (1)$$

where β was the angle between the C – H vector and bilayer normal. Experimentally, the order of C – ^{2}H vectors are determined by measuring the quadropolar splitting between the peaks of the powder spectrum and calculating the S_{CD} as follows

$$S_{CD} = \frac{4}{3}\Delta\nu_Q / A_Q \quad (2)$$

where $\Delta\nu_Q$ was the quadropolar splitting and $A_Q$was the quadropolar coupling constant. The electron density profile (EDP) was calculated using a binned method along the bilayer normal. The thickness of the membrane, *Z*, was calculated as the peak-to-peak distance of the total EDP in each leaflet. The hydrophobic core thickness, *D*, was measured as the peak-to-peak distance of the carbonyl EDP in each leaflet.

The compressibility modulus is a measure of the stiffness of the membrane and was calculated as,

$$K_A = k_B T \cdot A/\sigma_A^2 \quad (3)$$

where k_B was the Boltzmann constant, T was the temperature, A was the area, and σ_A^2 was the variance of the area during the simulation. The compression energy density (CED) of the bilayer illustrates the amount of energy necessary to compress or expand the membrane and was defined as,

$$CED = \frac{1}{2} K_A (d - d_0/d_0)^2 \quad (4)$$

where d was the thickness of the perturbed bilayer, and d_0 was the average bilayer thickness.

3. Results

During the course of all the simulations, the surface area per lipid remained fairly constant. The Top6 membrane had a surface area per lipid of 64 ± 1 Å^2. The POPE/POPG membrane was slightly denser with a surface area per lipid of 60 ± 1 Å^2 per lipid. The mixing of PE and PG lipids is unlikely to be inhomogeneous because PG lipids are negatively charged and repel each other.

To evaluate how well the ring moiety was parameterized in the cyclic lipids, we compared the calculated S_{CD} profile of PMPE with experiment. The quadrupolar splitting of a PE cy19:0/16:0 (PDSPE) lipid (at *sn*-2 carbon 5, 9, 10, and 16 positions) at 40 °C [27] and PC cy19:0/16:0 (PDSPC) lipid (at *sn*-2 carbon 2, 5, 8–11, 16, and 19 positions) at 40 °C [28] were measured experimentally (Fig. 2). The effect of the longer *sn-2* acyl change was assumed to be negligible. The S_{CD}s from the cy19 PE lipid matched very well with our calculated parameters for C5 and C9. Conversely, we underestimate the C10 order by 0.04. Still, we matched the trend that C10 is more disordered than the C9, which is different from the behavior of a double bond. The S_{CD}s at the 16 position did not match because PMPE consists of a terminating methyl group at that position where as the cy19 PE lipid consists of a methylene group.

Comparing the S_{CD}s of the cy19 PC lipid to cy19 PE lipid, we noticed the cy19 PC parameters were shifted down. We concluded that the S_{CD}s from the PC lipid would underestimate the order profile of the PMPE, but general patterns would be consistent, specifically the existence of S_{CD} splitting at C8, C17, and C11. Our calculated S_{CD}s at these positions did not show statistical splitting, but did match with at least one of the C–H vectors. Taking into account a larger head group and longer acyl chain, we feel our computed S_{CD} profile matches the pattern observed from experiment.

It is also worthy to note that Dufourc measured the effect of the cyclopropane ring on the phase transition from a bilayer to a hexagonal phase. In PE lipids, it reduces the transition temperature from between 55 and 75 °C to 38 and 58 °C [28]. According to Dufourc [28], at 40 °C, nearly all of the cyclic lipid system was in the bilayer phase. Also, we would like to enforce that no evidence of a phase transition during our short simulations was observed.

Double bonds are well known to induce local disordering as observed in the order profile of POPE (Fig. 3). Before the double bond, the average order parameter of C3–C7 was 0.21. A sharp decrease in the order parameter to an average of 0.075 is seen at the double bond, C9 and C10. The effect of the double bond is also seen in its adjacent carbons, C8 and C11 where the average order parameter is 0.1. The general order profile of PMPE was similar to POPE but there were notable differences in the ring region. The average order parameter of C3–C7 before the ring was 0.21 and C10 in the ring was 0.075, both similar to POPE. However, the order parameter of C9 in the ring was 0.15 and the adjacent carbons of the ring (C8 and C11) were similarly disordered as their neighboring ring carbons, a marked contrast from POPE. Also, the branched carbon of the ring C17 was of equal order as C9.

Overall the EDPs of the membranes had the same general shape. The profile consisted of the density of bulk water ($z > 30$ Å), the phospholipid head groups ($z \sim 17$–21 Å), the carbonyls ($z \sim 17$–21 Å), the double bonds and rings ($z \sim 5$–10 Å), and the tail ends of the lipids ($z \sim 0$) (Fig. 4). Component density peak location and distribution width as fitted by Gaussians are listed in Table 3. The peak-to-peak distances indicate the Top6 membrane is slightly thinner than the POPE/POPG membrane. The thickness, Z, of the Top6 membrane was 37.3 ± 0.2 Å while the POPE/POPG membrane was 40.1 ± 0.1 Å. The hydrophobic core thickness, D, of the Top6 and POPE/POPG membranes were 29.8 ± 0.1 and 32.7 ± 0.3 Å respectively. The POPE/POPG membrane was thicker than the Top6 membrane due to the longer lipids.

The length of the hydrophobic region of each lipid in the Top6 membrane was surprisingly similar given the varying lengths of the acyl chains. Thus, the longer lipids were either compressing or interdigitizing. The hydrophobic chain thickness of POPE in the POPE/POPG membrane was 32.7 ± 0.3 Å, but in the Top6 membrane it was 29.9 ± 0.6 Å. However the distance between C2 and C18 atoms in POPE in both the POPE/POPG and Top6 membranes was the same,

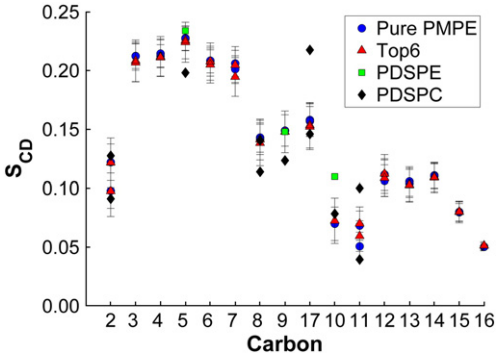

Fig. 2. PMPE S_{CD} profile. S_{CD} of *sn-2* chain of PMPE in the pure PMPE membrane (*blue circles*), PMPE in the Top6 membrane (*red triangles*), PDSPE from experiment at 40 °C [28] (*green squares*), and PDSPC from experiment at 40 °C [27] (*black diamonds*) The S_{CD} of PDSPE and PDSPC were calculated using equation 2 based on quadropolar splitting data and $A_Q = 170$ kHz [39] and 183 kHz [28] for sp3 hybridized (including C17) and cyclopropane (C9 and C10) carbons respectively. S_{CD} profiles of both chains in all the lipids of the Top6 membrane are shown in Fig. S3.

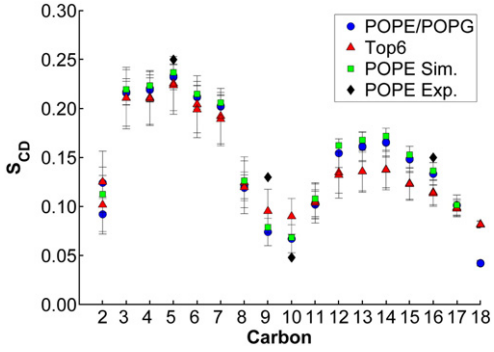

Fig. 3. POPE S_{CD} profile. S_{CD} of *sn-2* chain of POPE in the POPE/POPG membrane (*blue circles*), in the Top6 membrane (*red triangles*), from an NPT simulation with the C36 force field of a pure POPE membrane at 40 °C [26] (*green squares*), and from experiment of a pure POPE bilayer at 40 °C [40] (*black diamonds*).

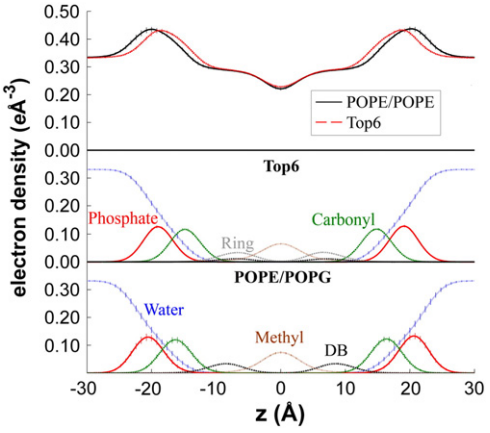

Fig. 4. Total electron densities (top), Top6 Component Densities (middle) and POPE/POPG Component Densities (bottom). The Top6 membrane is thinner than the POPE/POPG membrane. Water (*dotted blue*), phosphate (*solid red*), carbonyl (*dashed green*), ring (*dash dotted gray*), double bond (DB) (*dash dotted black*), and methyl (*dotted brown*) component EDP curves are labeled and are the same for both middle and bottom panels.

about 16 Å, indicating the lipids were not compressing. The level of leaflet interdigitizing is small though, as apparent in the single peak observed in the methylene group electron density profile of POPE in the Top6 membrane. The protrusion of methyl groups across the opposing bilayer's average PMPE methylene position in the Top6 membrane was calculated to be 0.5 ± 1 Å. As opposed to the POPE/POPG membrane where there was no protrusion, but a space of about 0.3 ± 0.2 Å.

The K_A of the POPE/POPG and Top6 membranes were 0.25 ± 0.04 and 0.34 ± 0.04 N/m respectively, thus the Top6 membrane is more rigid than the POPE/POPG membrane. Using the CED well (Fig. 5) and calculating the available thermal energy to be 0.001 J/nm^2 we estimated the POPE/POPG and Top6 bilayer thickness to thermally fluctuate between 36–44 and 35–40 Å respectively.

A summary of the Top6 and POPE/POPG membrane properties is given in Table 2.

4. Discussion and conclusion

A detailed *E. coli* membrane was developed to include a diverse set of lipids including species with a cyclic moiety. Initially, we attempted to use *cis* double bonded carbon parameters to describe the ring. However, inconsistencies with experimental S_{CD} parameters motivated us to develop QM-based parameters for the cyclic moiety. Most commonly, PE or in some cases PE/PG 18:1/16:0 lipids are used to model bacterial membranes, but the inclusion of lipids with a cyclic moiety produced noticeable changes in the surface density and stiffness of the membrane. Furthermore, the overall shorter acyl chain length of the Top6 membrane formed a thinner bilayer than the POPE/POPG membrane.

The main difference between the S_{CD} profile between the POPE and PMPE was the brief restoration of order between C9 and C10 (See Figs. 2 and 3). The *cis* double bond moiety effectively kinks the chain, which creates more volume for the C – H bonds to occupy and thereby decreasing the order of the chain at double bonds [29,30]. The kink orients the C9 – C10 bond in a direction nearly perpendicular to the bilayer normal, $90 \pm 1°$. The geometry of the ring also kinks the acyl chain because it prevents rotation around the C9 – C10 bond. As in POPE, the C9 – C10 bond is nearly perpendicular to the bilayer normal, $90 \pm 1°$. Thus the acyl chain order is decreased at the C9 and C10 in the cyclic moiety as well. However, the ring carbon, C17, is pushed into its chain and other chains, decreasing its available volume and thereby it is more ordered. Both lipids agreed with experimental order profiles of *E. coli* cells where local disordering was induced at the C10 position [31].

Table 2
Summary of membrane properties.

Membrane	SA [Å^2/lipid]	Z [Å]	D [Å]	K_A [N/m]
POPE/POPG	60 ± 1	40.1 ± 0.1	32.7 ± 0.3	0.25 ± 0.04
Top6	64 ± 1	37.3 ± 0.2	29.8 ± 0.1	0.34 ± 0.04

Table 3
Gaussian fits of EDP.

	POPE/POPG				Top6			
	Peak1		Peak2		Peak1		Peak2	
	μ_1	σ_1	μ_2	σ_2	μ_1	σ_1	μ_2	σ_2
Phosphate	20.6	2.4	-20.5	2.4	19.0	2.3	-19.0	2.3
Carbonyl	16.4	2.4	-16.3	2.4	14.8	2.3	-14.8	2.3
Ring	—	—	—	—	6.8	2.8	-6.8	2.9
Double bond	8.6	2.8	-8.5	2.8	7.2	3.0	-7.1	2.9
Methyl	0.0	3.1	—	—	0.0	3.3	—	—

All units in Å.

The protruding stable carbon also increased the surface area of PMPE (See Table 2). In broad terms, cyclic moieties decrease the surface density of lipids much like branched lipids [7]. A less dense bilayer could also allow for increased protein dynamics. The protruded carbon topology of cyclic moieties may also stabilize proteins better by fitting into crevices between folds.

The hydrophobic thickness of the membrane directly influences membrane and protein interaction and the tilt of the protein in the membrane. Negative hydrophobic mismatches, when the hydrophobic length of the protein is less than the membrane, causes local lipid deformations surrounding the protein to adjust to the hydrophobic length of the tilted protein. Positive hydrophobic mismatches, the hydrophobic length of the protein is greater than the membrane, mostly influences the tilt angle of the protein only [32]. A survey of *E. coli* cytosolic membrane proteins with significant transmembrane portions in the Orientations of Proteins in Membranes database (OPM) [33] shows that the average hydrophobic thickness is 29.4 ± 1 Å. The OPM database orients (rotation, depth, and tilt) proteins in an implicit, adjustable thickness, anistropic solvent model of a lipid bilayer. The POPE/POPG membrane hydrophobic thickness is slightly greater where as the Top6 membrane agrees very well with the OPM survey (See Table 2).

The energetic cost associated with deforming the membrane to match the hydrophobic length is mostly to due to compression/expansion of the bilayer and bending of the monolayer. The monolayer

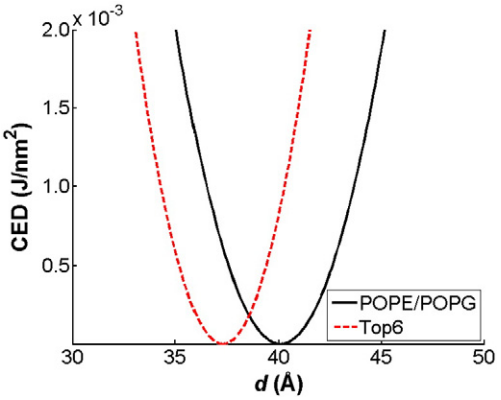

Fig. 5. Compression energy density. The POPE/POPG (*black solid*) and Top6 (*red dashed*) membranes are likely to fluctuate between 36–44 and 35–40 Å in thickness respectively.

bending modulus is a function of the lipid head group size and the PE: PG is similar in the POPE/POPG and Top6 membranes. Therefore, we assumed the energetic cost due to bending of the monolayer was similar for the POPE/POPG and Top6 membranes. The K_A is a function of the surface area per lipid of the membrane. Thus, the Top6 membrane had a larger K_A and was slightly harder to compress/expand (See Table 2). However, the hydrophobic thickness of the Top6 membrane matches the calculated hydrophobic length of *E. coli* transmembrane proteins so it can afford to be more rigid. The flexibility of the POPE/POPG membrane allows for compression to match the hydrophobic length of transmembrane proteins found in *E. coli* at a minimal cost of 200–250 J/mol (See Fig. 5).

The Top6 membrane will likely be beneficial in several areas of *E. coli* membrane MD research such as antimicrobial peptides (AMPs), proteins which are regulated by the membrane and integral membrane proteins which undergo large conformational changes. AMPs are membrane associated proteins which insert into the membrane to kill bacteria. It is believed that they insert into the membrane unfolded where secondary structure is then induced [34]. The insertion process, which perturbs the membrane, could be affected by the compressibility and surface area per lipid of the membrane. AMPs then kill the bacteria by permeabilizing the membrane by forming pores across the membrane, which depends on the thickness of the membrane. Cirac et al. [34] performed MD simulations using a DPPG bilayer described by a GROMOS96 based force field to understand the molecular basis of how AMPs functions. It is very conceivable that the molecular interactions could change upon using a more accurate membrane.

The complex membrane should also be beneficial in understanding the interactions between membranes and membrane regulated proteins such as *E. coli* mechanosensitive channels (MscL and MscS). These channels serve as turgor pressure release valves and open or close in response to tension in the membrane. Wiggins and Phillips have estimated that the bilayer thickness deformation due to hydrophobic mismatching is important in gating of MscS [4]. In fact, Perozo et al. performed experiments where decreasing the bilayer thickness decreased the activation energy of MscL [35]. Thus, the compressibility and thickness of the membrane help regulate the opening and closing of these channels. Explicit membrane MD studies of MscS have used POPE bilayers described by a GROMOS FF [36] and POPC bilayers described by a CHARMM27 FF [37,38]. The use of these simple membranes may produce artifacts which would not be seen with a more accurate membrane.

A detailed *E. coli* membrane has been developed for use in MD simulations. The composition of the bilayer was fit to a several experimentally determined compositions of *E. coli* and consisted of six different lipids, including lipids with a cyclic moiety near the center of the chain. QM-based parameters were developed to describe the cyclopropane ring within the acyl chain to match deuterium order parameters. The complex membrane was simulated along with simple POPE/POPG and pure PMPE membranes. It was found that the complex membrane matched the hydrophobic length of integral *E. coli* membrane proteins better than the POPE/POPG membrane. The complex membrane was also less dense and slightly more rigid. To our knowledge, the complex Top6 membrane is the most accurate representation of an *E. coli* cytoplasmic lipid bilayer. We believe that more accurate simulations are possible with a diverse population of lipids and suggest the use of the Top6 membrane as opposed to simple POPE or POPE/POPG membranes for MD simulations of *E. coli* membranes

Acknowledgments

This research was supported in part by the National Science Foundation through TeraGrid (now XSEDE) resources provided by National Institute for Computational Sciences (Kraken) under grant number TG-MCB100139 and the High Performance Computing Cluster at the University of Maryland.

Appendix A. Supplementary data

Supplementary data to this article can be found online at doi:10.1016/j.bbamem.2012.01.009.

References

[1] J.-L. Popot, Amphipols, nanodiscs, and fluorinated surfactants: three nonconventional approaches to studying membrane proteins in aqueous solutions, Annu. Rev. Biochem. 79 (2010) 737–775.
[2] R. Krämer, C. Ziegler, Regulative interactions of the osmosensing C-terminal domain in the trimeric glycine betaine transporter BetP from *Corynebacterium glutamicum*, Biol. Chem. 390 (2009) 685–691.
[3] M.F. Lensink, C. Govaerts, J.-M. Ruysschaert, Identification of specific lipid-binding sites in integral membrane proteins, J. Biol. Chem. 285 (2010) 10519–10526.
[4] P. Wiggins, R. Phillips, Membrane–protein interactions in mechanosensitive channels, Biophys. J. 88 (2005) 880–902.
[5] O.K. Dalrymple, W. Isaacs, E. Stefanakos, M.A. Trotz, D.Y. Goswami, Lipid vesicles as model membranes in photocatalytic disinfection studies, J. Photochem. Photobiol. A 221 (2011) 64–70.
[6] S. Jo, J.B. Lim, J.B. Klauda, W. Im, CHARMM-GUI membrane builder for mixed bilayers and its application to yeast membranes, Biophys. J. 97 (2009) 50–58.
[7] J.B. Lim, J.B. Klauda, Lipid chain branching at the iso- and anteiso-positions in complex chlamydia membranes: a molecular dynamics study, Biochim. Biophys. Acta 1808 (2011) 323–331.
[8] R. Alhadeff, A. Ganoth, M. Krugliak, I.T. Arkin, Promiscuous binding in a selective protein: the bacterial Na^+/H^+ antiporter, PLoS One 6 (2011) e25182.
[9] S. Jo, T. Kim, V.G. Iyer, W. Im, CHARMM-GUI: a web-based graphical user interface for CHARMM, J. Comput. Chem. 29 (2008) 1859–1865.
[10] S. Morein, A.-S. Andersson, L. Rilfors, G. Lindblom, Wild-type *Escherichia coli* cells regulate the membrane lipid composition in a window between gel and non-lamellar structures, J. Biol. Chem. 271 (1996) 6801–6809.
[11] K. Murzyn, M. Pasenkiewicz-Gierula, Construction and optimisation of a computer model for a bacterial membrane, Acta Biochim. Pol. 46 (1999) 631–639.
[12] W. Zhao, T. Róg, A.A. Gurtovenko, I. Vattulainen, M. Karttunen, Role of phosphatidylglycerols in the stability of bacterial membranes, Biochimie. 90 (2008) 930–938.
[13] E.J. Dufourc, I.C.P. Smith, H.C. Jarrell, The role of cyclopropane moieties in the lipid properties of biological membranes: a deuterium NMR structural and dynamical approach, Biochemistry 23 (1984) 2300–2309.
[14] D. Grogan, J. Cronan, Cyclopropane ring formation in membrane lipids of bacteria, Microbiol. Mol. Biol. Rev. 61 (1997) 429–441.
[15] L.O. Ingram, Changes in lipid composition of *Escherichia coli* resulting from growth with organic solvents and with food additives, Appl. Environ. Microbiol. 33 (1977) 1233–1236.
[16] D. Oursel, C. Loutelier-Bourhis, N. Orange, S. Chevalier, V. Norris, C.M. Lange, Lipid composition of membranes of *Escherichia coli* by liquid chromatography/tandem mass spectrometry using negative electrospray ionization, Rapid Commun. Mass Spectrom. 21 (2007) 1721–1728.
[17] Y. Ishida, K. Kitagawa, A. Nakayama, H. Ohtani, Complementary analysis of lipids in whole bacteria cells by thermally assisted hydrolysis and methylation-GC and MALDI-MS combined with on-probe sample pretreatment, J. Anal. Appl. Pyrolysis 77 (2006) 116–120.
[18] E. Mileykovskaya, W. Dowhan, Visualization of phospholipid domains in *Escherichia coli* by using the cardiolipin-specific fluorescent dye 10-N-nonyl acridine orange, J. Bacteriol. 182 (2000) 1172–1175.
[19] B.R. Brooks, C.L. Brooks III, A.D. Mackerell Jr., L. Nilsson, R.J. Petrella, B. Roux, et al., CHARMM: the biomolecular simulation program, J. Comput. Chem. 30 (2009) 1545–1614.
[20] J.C. Phillips, R. Braun, W. Wang, J. Gumbart, E. Tajkhorshid, E. Villa, et al., Scalable molecular dynamics with NAMD, J. Comput. Chem. 26 (2005) 1781–1802.
[21] T. Darden, D. York, L. Pedersen, Particle mesh Ewald: an N·log(N) method for Ewald sums in large systems, J. Chem. Phys. 98 (1993) 10089.
[22] J.-P. Ryckaert, G. Ciccotti, H.J.C. Berendsen, Numerical integration of the cartesian equations of motion of a system with constraints: molecular dynamics of n-alkanes, J. Comput. Phys. 23 (1977) 327–341.
[23] W.G. Hoover, Canonical dynamics: equilibrium phase-space distributions, Phys. Rev. A 31 (1985) 1695.
[24] S. Nosé, A study of solid and liquid carbon tetrafluoride using the constant pressure molecular dynamics technique, J. Chem. Phys. 78 (1983) 6928.
[25] S.E. Feller, Y. Zhang, R.W. Pastor, B.R. Brooks, Constant pressure molecular dynamics simulation: the Langevin piston method, J. Chem. Phys. 103 (1995) 4613.
[26] J.B. Klauda, R.M. Venable, J.A. Freites, J.W. O'Connor, D.J. Tobias, C. Mondragon-Ramirez, et al., Update of the CHARMM all-atom additive force field for lipids: validation on six lipid types, J. Phys. Chem. B 114 (2010) 7830–7843.

[27] B. Perly, I.C.P. Smith, H.C. Jarrell, Effects of the replacement of a double bond by a cyclopropane ring in phosphatidylethanolamines: a deuterium NMR study of phase transitions and molecular organization, Biochemistry 24 (1985) 1055–1063.
[28] E.J. Dufourc, I.C.P. Smith, H.C. Jarrell, A ^{2}H-NMR analysis of dihydrosterculoyl-containing lipids in model membranes: structural effects of a cyclopropane ring, Chem. Phys. Lipids 33 (1983) 153–177.
[29] J. Seelig, N. Waespe-Sarcevic, Molecular order in cis and trans unsaturated phospholipid bilayers, Biochemistry 17 (1978) 3310–3315.
[30] S.P. Soni, J.A. Ward, S.E. Sen, S.E. Feller, S.R. Wassall, Effect of trans unsaturation on molecular organization in a phospholipid membrane, Biochemistry 48 (2009) 11097–11107.
[31] H.U. Gally, G. Pluschke, P. Overath, J. Seelig, Structure of *Escherichia coli* membranes. Phospholipid conformation in model membranes and cells as studied by deuterium magnetic resonance, Biochemistry 18 (1979) 5605–5610.
[32] T. Kim, W. Im, Revisiting hydrophobic mismatch with free energy simulation studies of transmembrane helix tilt and rotation, Biophys. J. 99 (2010) 175–183.
[33] M.A. Lomize, A.L. Lomize, I.D. Pogozheva, H.I. Mosberg, OPM: orientations of proteins in membranes database, Bioinformatics 22 (2006) 623–625.
[34] A.D. Cirac, G. Moiset, J.T. Mika, A. Koçer, P. Salvador, B. Poolman, et al., The molecular basis for antimicrobial activity of pore-formingcyclic peptides, BPJ 100 (2011) 2422–2431.
[35] E. Perozo, A. Kloda, D.M. Cortes, B. Martinac, Physical principles underlying the transduction of bilayer deformation forces during mechanosensitive channel gating, Nat. Struct. Mol. Biol. 9 (2002) 696–703.
[36] S.A. Spronk, D.E. Elmore, D.A. Dougherty, Voltage-dependent hydration and conduction properties of the hydrophobic pore of the mechanosensitive channel of small conductance, Biophys. J. 90 (2006) 3555–3569.
[37] A. Anishkin, K. Kamaraju, S. Sukharev, Mechanosensitive channel MscS in the open state: modeling of the transition, explicit simulations, and experimental measurements of conductance, J. Gen. Physiol. 132 (2008) 67–83.
[38] M. Sotomayor, V. Vásquez, E. Perozo, K. Schulten, Ion conduction through MscS as determined by electrophysiology and simulation, Biophys. J. 92 (2007) 886–902.
[39] L.J. Burnett, Deuteron quadrupole coupling constants in three solid deuterated paraffin hydrocarbons: C2D6, C4D10, C6D14, J. Chem. Phys. 55 (1971) 5829.
[40] B. Perly, I.C. Smith, H.C. Jarrell, Acyl chain dynamics of phosphatidylethanolamines containing oleic acid and dihydrosterculic acid: ^{2}H NMR relaxation studies, Biochemistry 24 (1985) 4659–4665.